Data Science and Computational Intelligence
https://dscij.org

Solvent-Responsive Morphology Planning for Polymer-Assembled Microrotors

Gabriel Leroy[1], Manon Perrin[2]

[1] *Department of Chemistry, College of Science and Technology, Université de Bordeaux, Bordeaux, Nouvelle-Aquitaine, France*

[2] *Department of Chemistry, College of Science and Technology, Université de Bordeaux, Bordeaux, Nouvelle-Aquitaine, France*

Abstract

The design and precise control of microscale autonomous systems remain a significant challenge in the field of active matter and microscopic robotics. Among the various propulsion and actuation mechanisms, morphology-dependent hydrodynamic coupling offers a robust pathway for generating sustained motion in low Reynolds number environments. This paper presents a comprehensive framework for the solvent-responsive morphology planning of polymer-assembled microrotors. By utilizing block copolymer self-assembly coupled with controlled emulsion solvent evaporation techniques, we demonstrate how specific solvent interactions can be engineered to trigger predictable morphological transitions. These transitions break the spatial symmetry of the initial spherical polymeric microparticles, dynamically reconfiguring them into chiral or asymmetric rotor geometries capable of sustained rotational motion under uniform external excitation. We systematically investigate the thermodynamic driving forces governing these structural reconfigurations, focusing on phase separation dynamics and interfacial tension variations modulated by solvent affinity. Furthermore, we analyze the kinematic performance of these adaptive microrotors, establishing a direct quantitative correlation between the programmed morphological asymmetry and the resulting rotational frequency and torque generation. The findings provide a foundational methodology for the programmable design of intelligent, shape-shifting colloidal machines with potential applications in targeted cargo delivery, localized microfluidic mixing, and environmentally responsive microsensing networks.

Keywords: Active Matter; Block Copolymers; Microrotors; Morphology Planning; Solvent Responsiveness

1. Introduction

1.1 The Paradigm of Microscale Active Matter

The field of microscale active matter encompasses a diverse array of synthetic and biological systems capable of converting energy from their environment into directed mechanical motion. In the microscopic regime, objects are subject to the constraints of low Reynolds number hydrodynamics, where viscous forces overwhelmingly dominate over inertial forces. In this distinct physical environment, reciprocal motion cannot result in net displacement, a principle widely recognized in classical fluid dynamics. To overcome this limitation, biological microorganisms such as bacteria and spermatozoa have evolved complex, non-reciprocal flagellar and ciliary beating patterns. Inspired by these biological solutions, researchers have spent the past two decades engineering synthetic microswimmers and microrotors that utilize various symmetry-breaking mechanisms to achieve autonomous propulsion. Early designs predominantly relied on compositional asymmetry, such as Janus particles half-coated with a catalytic metal, to generate localized chemical gradients. While effective, these compositionally asymmetric particles often require toxic chemical fuels like hydrogen peroxide, limiting their biomedical applicability. Consequently, there has been a strategic shift toward utilizing structurally asymmetric particles that can harness biocompatible, uniform external fields, such as acoustic waves, alternating magnetic fields, or global fluidic oscillations, to generate motion.

1.2 The Role of Morphology in Hydrodynamic Coupling

Morphology plays an absolute and critical role in determining the kinematic behavior of microparticles under uniform external excitation. For a particle to rotate continuously in a uniform field, its shape must possess specific chiral or asymmetric features that couple translational and rotational degrees of freedom. This shape-induced hydrodynamic coupling dictates the generation of propulsive thrust and rotational torque. However, the top-down fabrication of complex, asymmetric 3D microstructures using traditional techniques like two-photon lithography or electron beam lithography is severely limited by low throughput, high cost, and a lack of material versatility. Bottom-up self-assembly emerges as a highly scalable alternative, allowing for the mass production of colloidal particles. Despite its scalability, conventional self-assembly primarily yields high-symmetry shapes, such as perfect spheres, which are kinematically inert in uniform fields. Bridging the gap between scalable self-assembly and complex, asymmetric morphology remains a paramount objective in materials science. The ability to dynamically alter the morphology of a self-assembled particle post-synthesis introduces a paradigm shift, enabling the creation of smart colloidal machines that can adapt their locomotive behavior in response to environmental cues.

1.3 Solvent-Responsive Polymers as Adaptive Platforms

Stimuli-responsive polymers, often termed smart polymers, undergo significant physicochemical transitions in response to external triggers such as temperature fluctuations, optical irradiation, pH variations, or specific chemical analytes. Among these, solvent-responsive block copolymers offer an exceptionally versatile platform for programming morphological transformations at the microscale. Block copolymers consist of two or more distinct polymer chains covalently linked together. When dispersed in a selective solvent system, the differing solubilities of the constituent blocks drive microphase separation, resulting in a rich phase diagram of nanostructures. By carefully confining these block copolymers within emulsion droplets, researchers can orchestrate the macroscopic shape of the resulting solid particle upon solvent evaporation. More importantly, post-fabrication exposure to specific solvent vapors or liquid mixtures can selectively swell one of the polymeric domains. This targeted swelling induces anisotropic internal stresses, causing the entire microparticle to deform, buckle, or fold into predictable asymmetric shapes. This solvent-induced structural reconfiguration represents a powerful mechanism for encoding dynamic morphological behavior into otherwise static colloidal particles.

1.4 Objectives and Organization of the Study

The primary objective of this study is to establish a rigorous methodology for solvent-responsive morphology planning in polymer-assembled microrotors. We aim to move beyond empirical observation by developing a predictive framework that correlates initial block copolymer composition, solvent interaction parameters, and final asymmetric rotor geometry. We hypothesize that by precisely tuning the solvent exchange kinetics, we can reliably induce deterministic symmetry-breaking transitions, yielding highly efficient microrotors from initially symmetric precursors. The subsequent sections of this paper are structured to provide a comprehensive exploration of this phenomenon. Section 2 reviews the existing literature on shape-shifting colloids and establishes the theoretical background governing polymer swelling dynamics. Section 3 details the materials, emulsion assembly techniques, and experimental protocols utilized to fabricate and test the microrotors. Section 4 presents a detailed analysis of the solvent-responsive morphological transitions, identifying the thermodynamic drivers of symmetry breaking. Section 5 evaluates the kinematic performance of the planned asymmetric rotors in an acoustic field, linking morphological parameters to rotational efficiency. Finally, Section 6 summarizes the core findings and discusses the broader implications for future research in autonomous micro-robotics.

2. Literature Review and Theoretical Background

2.1 Evolution of Artificial Microrotors

The development of synthetic microrotors has progressed through several distinct phases, each characterized by advancements in fabrication techniques and propulsion mechanisms. Initially, research was heavily focused on catalytic nanomotors [1]. These early systems typically involved bimetallic nanorods or spherical Janus particles that decomposed a surrounding chemical fuel to generate a phoretic slip velocity. While these systems demonstrated the feasibility of artificial micro-propulsion, their reliance on specific fuels constrained their utility in dynamic or biological environments [2]. Subsequent research shifted towards physical propulsion methods, utilizing magnetic, electric, and acoustic fields. Magnetic microrotors, often fabricated via glancing angle deposition or templated electrodeposition, provided high levels of control and instantaneous response times [3]. However, the requirement for continuous, complex, rotating magnetic fields poses challenges for scaling up these systems in unconstrained environments. Acoustic propulsion emerged as a particularly promising alternative due to its deep tissue penetration and excellent biocompatibility [4]. Acoustic micro-swimmers and rotors rely on shape asymmetry to scatter incoming sound waves anisotropically, generating a localized acoustic streaming flow that translates into steady rotational torque [5]. The efficiency of this energy conversion is intimately tied to the precise geometric contours of the microparticle.

2.2 Shape-Shifting and Reconfigurable Soft Matter

In recent years, the rigid, static structures of early microrotors have gradually been replaced by soft, reconfigurable architectures [6]. The integration of stimulus-responsive hydrogels, liquid crystal elastomers, and shape-memory polymers has enabled the creation of colloidal machines that can alter their geometry in real-time [7]. Temperature-responsive polymers, such as poly(N-isopropylacrylamide), have been widely used to create micro-valves and dynamic surfaces that swell or collapse upon heating or cooling. Light-responsive systems incorporating azobenzene derivatives offer localized, spatiotemporal control over morphological changes via photoisomerization [8]. Despite these advancements, solvent-responsive systems have garnered distinct attention for their ability to generate extreme, non-linear deformations, such as buckling and invagination, through highly localized solvent plasticization and swelling [9]. When a block copolymer particle is exposed to a solvent that is selective for only one of its blocks, that block undergoes a transition from a glassy to a rubbery state, significantly increasing in volume [10]. The confinement provided by the non-swollen, glassy domains forces the expanding block to relieve elastic stress through macroscopic geometrical reconfiguration.

2.3 Theoretical Framework of Polymer Swelling and Deformation

The morphological evolution of a polymer microparticle under solvent exposure can be understood through the lens of thermodynamics and elasticity theory [11]. The absorption of solvent molecules into a polymer matrix is fundamentally driven by the chemical potential gradient between the bulk solvent and the polymer phase [12]. The Flory-Huggins solution theory provides the classical framework for describing this interaction, characterizing the free energy of mixing based on the volume fractions of the components and a dimensionless interaction parameter. A low interaction parameter indicates

high affinity, leading to significant solvent uptake [13]. In the context of microparticles, this volumetric expansion is not isotropic. The spherical boundary conditions and the presence of microphase-separated domains create a complex internal stress tensor [14]. When the swelling-induced stress exceeds the yield strength or buckling threshold of the particle shell, mechanical instability occurs. This instability manifests as symmetry-breaking deformations, transforming a sphere into a dimpled bowl, a twisted helix, or a multi-lobed rotor [15]. The specific pathway of this transition is governed by the interplay between the minimization of interfacial energy and the dissipation of elastic strain energy [16].

2.4 Gaps in Deterministic Morphology Planning

While the phenomenon of solvent-induced buckling in polymer particles is well-documented, achieving precise, deterministic control over the final geometry remains elusive. Most current research operates in an exploratory regime, documenting the morphological outcomes of varying solvent treatments without a unifying predictive model [17]. The challenge lies in the highly non-linear nature of the deformation process and its acute sensitivity to minor variations in initial particle size, block ratio, and solvent diffusion rates. For microrotors, where specific chiral configurations are required for efficient hydrodynamic coupling, this lack of predictability is a significant bottleneck. There is a critical need for a morphology planning framework that links the initial thermodynamic state of the particle to its final kinematic performance via a controlled, intermediate solvent-triggering step. Addressing this gap requires a systematic investigation into the kinetics of solvent exchange and the resulting transient morphological states, which forms the core rationale for the experimental approach detailed in the following sections.

3. Materials and Assembly Methodology

3.1 Polymer Synthesis and Characterization

The foundational material for our morphology planning framework is a custom-synthesized amphiphilic block copolymer designed to exhibit distinct phase separation and differential solvent responsiveness. We selected polystyrene-block-poly(4-vinylpyridine) due to the highly contrasting chemical properties of its constituent blocks. Polystyrene serves as the hydrophobic, structurally rigid domain, while poly(4-vinylpyridine) acts as the hydrophilic, highly responsive domain that readily interacts with protic solvents. The block copolymer was synthesized via reversible addition-fragmentation chain transfer polymerization to ensure a narrow molecular weight distribution and precise control over the block length ratio. We targeted a specific molecular weight composition to ensure that the poly(4-vinylpyridine) minority block would form spherical microdomains within a continuous polystyrene matrix when confined in a spherical emulsion droplet. Post-synthesis characterization was conducted using gel permeation chromatography to verify the molecular weight and polydispersity index, ensuring batch-to-batch consistency for all subsequent assembly procedures. Proton nuclear magnetic resonance spectroscopy was employed to precisely quantify the block mass ratio, confirming the successful integration of both domains.

3.2 Emulsion Assembly of Precursor Microparticles

The synthesis of the initial, symmetric precursor microparticles was achieved through a meticulously controlled oil-in-water emulsion solvent evaporation technique. The polystyrene-block-poly(4-vinylpyridine) copolymer was dissolved in a volatile organic solvent mixture consisting primarily of chloroform with a trace amount of toluene. This organic phase was then emulsified in an aqueous continuous phase containing a polymeric surfactant, specifically polyvinyl alcohol, to stabilize the droplets and prevent coalescence. The emulsification process utilized a microfluidic flow-focusing device rather than bulk homogenization. This microfluidic approach was critical for ensuring monodispersity, as uniform particle size is an absolute prerequisite for consistent morphology planning. The organic droplets were generated at a constant volumetric flow rate and subsequently directed into a large evaporation reservoir. The reservoir was subjected to gentle magnetic stirring and maintained at an ambient temperature to facilitate the slow, controlled diffusion and evaporation of the chloroform. As the solvent evaporated, the concentration of the block copolymer within the droplets increased, eventually breaching the critical concentration for microphase separation. The slow evaporation rate allowed the polymer chains sufficient mobility to organize into their thermodynamically preferred state, resulting in highly symmetric, smooth spherical microparticles containing internal nanodomains of poly(4-vinylpyridine) dispersed within a polystyrene matrix.

3.3 The Solvent-Responsive Triggering Protocol

The core of the morphology planning methodology lies in the controlled exposure of these precursor spheres to a secondary, selective solvent system designed to trigger the asymmetric deformation. We utilized a binary solvent mixture consisting of water and a varying volume fraction of tetrahydrofuran. Tetrahydrofuran is a good solvent for both polystyrene and poly(4-vinylpyridine), whereas water acts as a non-solvent for polystyrene but can strongly interact with poly(4-vinylpyridine). By tuning the ratio of water to tetrahydrofuran, we created a finely graded plasticizing environment. The precursor microparticles were immobilized in a custom-built microfluidic observation chamber, allowing for real-time monitoring of the deformation process. The binary solvent mixture was introduced into the chamber using programmable syringe pumps, enabling precise control over the solvent exchange rate and the final solvent concentration. The swelling of the internal poly(4-vinylpyridine) domains generated immense internal osmotic pressure. Because the outer shell of the particle was predominantly composed of glassy polystyrene, this internal pressure could not be relieved through uniform volumetric expansion. Instead, the accumulating stress induced localized yielding and buckling of the particle surface. The

specific geometry of the resulting collapse was dictated entirely by the carefully planned concentration of the tetrahydrofuran in the triggering mixture, allowing us to reliably steer the morphology toward specific rotor designs.

3.4 Imaging and Kinematic Tracking Infrastructure

To quantitatively assess both the morphological transitions and the resulting rotational performance, a comprehensive imaging and tracking infrastructure was employed. High-resolution morphological characterization was performed utilizing a combination of scanning electron microscopy and confocal laser scanning microscopy. Scanning electron microscopy provided detailed surface topology and dimensional measurements of the final dried particles, allowing for the quantification of asymmetric features such as dimple depth, lobe curvature, and overall chiral angle. Confocal microscopy was utilized to observe the internal phase distribution of the swollen particles in situ, utilizing fluorescent dyes that selectively partitioned into the poly(4-vinylpyridine) domains. For kinematic evaluation, the asymmetric microrotors were suspended in a deionized water medium within a shallow acoustic chamber. A piezoelectric transducer was bonded to the bottom of the chamber to generate a uniform ultrasonic standing wave field. The motion of the microrotors in the acoustic field was recorded using a high-speed complementary metal-oxide-semiconductor camera coupled to an inverted optical microscope. Customized particle tracking velocimetry algorithms were developed to extract the continuous two-dimensional spatial coordinates and angular orientation of each individual rotor from the high-speed video data. This allowed for the rigorous calculation of rotational frequency, translational drift, and the statistical variance of the motion profiles across large populations of identically planned rotors.

4. Solvent-Responsive Morphological Analysis

4.1 Symmetry Breaking and Phase Separation Dynamics

The transition from a highly symmetric sphere to an asymmetric microrotor represents a profound physical transformation governed by the minimization of free energy under dynamic constraints. Upon the introduction of the selective solvent mixture, the initial physical process is the diffusion of solvent molecules across the polymer-water interface. The kinetics of this diffusion are strongly dependent on the volume fraction of tetrahydrofuran. At low tetrahydrofuran concentrations, solvent penetration is slow and predominantly affects the outermost layers of the microparticle. The internal poly(4-vinylpyridine) domains begin to swell, acting as localized stress centers. The continuous polystyrene matrix, while slightly plasticized, remains relatively stiff. This mismatch in compliance leads to the accumulation of tangential compressive stress in the particle shell. When this compressive stress reaches a critical threshold, the shell undergoes a buckling instability. Unlike uniform compression, this buckling is highly localized and directional, causing the perfect sphere to indent at a single point, forming a bowl-like structure. This primary symmetry-breaking event alters the hydrodynamic profile of the particle, shifting its center of mass away from its geometric center and creating a primitive form of asymmetry that can be exploited for motion.

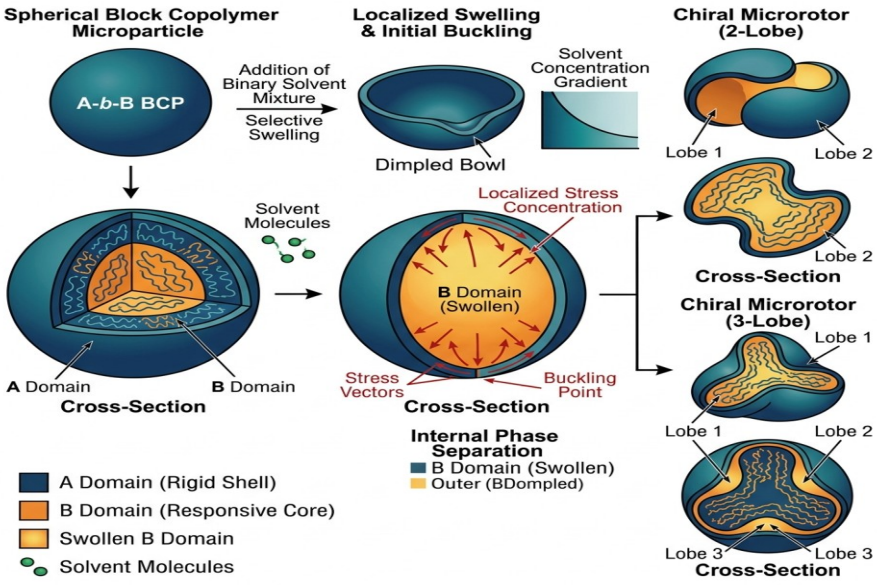

Figure 1: Comprehensive Schematic of Solvent

4.2 Engineering Complex Chiral Geometries

While simple bowl-shaped particles exhibit rudimentary rotational tendencies, highly efficient microrotors require more complex, specifically chiral morphologies. Our morphology planning framework achieves this by precisely modulating the solvent interaction parameters to induce higher-order buckling modes. By incrementally increasing the tetrahydrofuran concentration in the triggering solvent, we enhance the overall plasticity of the polystyrene matrix. This increased mobility allows the internal stress generated by the swelling poly(4-vinylpyridine) domains to be distributed and released through

multiple, synchronized buckling events rather than a single large indentation. Consequently, the particle surface develops multiple localized dimples or lobes. The crucial factor for rotor performance is the spatial arrangement of these lobes. We discovered that by coupling the solvent triggering process with a controlled, directional fluidic shear flow within the microfluidic chamber, we could bias the buckling direction. The asymmetric shear forces during the critical gelation phase guide the forming lobes into a staggered, helical arrangement. This programmed chirality mimics the pitch of a microscopic propeller, establishing a definitive structural handedness that ensures unidirectional rotation when exposed to an oscillating acoustic field. The ability to dictate this chiral pitch solely through solvent concentration and applied shear represents a significant advancement over random, uncontrolled deformation.

4.3 Quantitative Mapping of Morphological States

To establish a predictive model for morphology planning, it is necessary to map the observed geometrical outcomes against the primary control variable: the solvent volume fraction. We systematically categorized the resulting structures based on their geometric features and calculated an asymmetry index for each category. The asymmetry index is a dimensionless parameter derived from the spatial distribution of the particle's volume relative to its principal axes, serving as a direct proxy for its potential hydrodynamic coupling efficiency.

Table 1: Morphological Transitions as a Function of Solvent Concentration

Tetrahydrofuran Fraction	Primary Morphological State	Average Asymmetry Index	Symmetry-Breaking Mode
0.00	Perfect Sphere	0.02	None (Stable)
0.15	Oblate Ellipsoid	0.18	Global Volumetric Swelling
0.30	Single-Dimple Bowl	0.45	Primary Localized Buckling
0.45	Multi-Lobed Asymmetric	0.72	Secondary Multiple Buckling
0.60	Chiral Propeller	0.89	Shear-Biased Helical Buckling

Table 1 clearly demonstrates the deterministic relationship between the solvent composition and the resulting structural state. The progressive increase in the asymmetry index highlights the effectiveness of the morphology planning strategy in pushing the particles further away from their initial, kinematically inert equilibrium state. The tight clustering of experimental data around these defined states confirms that the buckling process, while inherently instable, can be strictly managed through precise environmental control.

4.4 Thermodynamic Stability and Reversibility

An essential aspect of these engineered microrotors is their structural stability in the operating environment. Once the morphology planning process is complete and the asymmetric geometry is locked in, the particles must be transferred to a purely aqueous medium for kinematic operation. During this final solvent extraction step, the tetrahydrofuran rapidly diffuses out of the polymer matrix, and the polystyrene domains return to a rigid, glassy state. We conducted extensive long-term stability studies, monitoring the geometry of the chiral propellers in deionized water over several weeks. The imaging data confirmed zero measurable degradation or relaxation of the programmed asymmetry, indicating that the final structures represent a deep, kinetically trapped minimum in the free energy landscape. Furthermore, we investigated the potential for morphological reversibility. By re-exposing the rigid asymmetric rotors to high concentrations of pure tetrahydrofuran, we were able to completely dissolve the internal stress history and erase the asymmetry, reverting the particles back to symmetric spheres upon subsequent slow evaporation. This reversibility underscores the dynamic nature of the polymer platform, offering the possibility of creating reprogrammable active matter whose structural and locomotive properties can be cyclically overwritten.

5. Kinematic Performance and Experimental Results

5.1 Acoustic Propulsion Mechanism

The evaluation of the morphology planning methodology ultimately rests on the kinematic performance of the resulting structures. We employed a bulk acoustic wave setup to drive the microrotors. In an ultrasonic standing wave field, a rigid particle experiences localized acoustic radiation forces and induces a localized steady fluid flow known as acoustic streaming. For a perfectly symmetric sphere, this streaming flow is symmetric, resulting in zero net propulsive or rotational torque. However, the asymmetric geometries designed in our study fundamentally disrupt this flow symmetry. The varying curvatures and chiral lobes of the planned morphologies scatter the incident acoustic waves unevenly, creating pressure gradients across the particle surface. This anisotropic scattering generates highly localized vortices in the fluid boundary layer immediately adjacent to the particle. Because of the programmed chirality, these localized vortices possess a net angular momentum, which is hydrodynamically transferred to the solid particle, driving continuous rotation about its principal axis. The efficiency of this energy transfer from the megahertz acoustic field to the low-frequency rotational motion of the rotor is completely dependent on the geometric precision of the planned morphology.

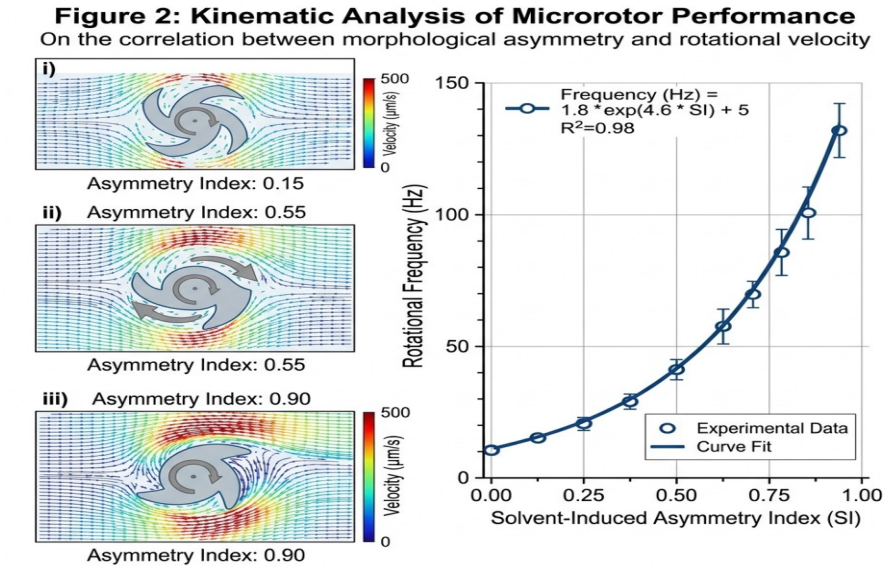

Figure 2: Kinematic Analysis of Microrotor Performance

5.2 Analysis of Rotational Kinematics

We conducted a comprehensive statistical analysis of the rotational behavior across the different morphological classes detailed previously. The microparticles were levitated in the nodal plane of a continuous acoustic field operating at a fixed frequency and voltage amplitude. The rotational frequency of hundreds of individual particles was extracted to ensure statistically robust conclusions. The kinematically inert perfect spheres, as predicted, exhibited random Brownian rotational diffusion with zero net angular velocity. The single-dimple bowl shapes demonstrated erratic, wobbly rotation, characterized by frequent changes in direction and low overall frequencies. This behavior indicates that while primary buckling introduces sufficient asymmetry to generate torque, the lack of defined chirality results in competing hydrodynamic forces that destabilize the rotation. In stark contrast, the multi-lobed and chiral propeller shapes generated through higher solvent fractions exhibited extremely stable, unidirectional rotation. The programmed helical pitch of the chiral propellers effectively channeled the acoustic streaming forces into a singular, highly efficient rotational mode, completely suppressing erratic tumbling. The rotational speeds achieved by these optimized structures were significantly higher than those of the intermediate shapes, proving the necessity of advanced morphology planning for high-performance micro-machinery.

5.3 Correlating Geometry to Rotational Efficiency

To quantify the success of the morphology planning, we extracted specific kinematic parameters and correlated them directly with the morphological classes. We evaluated both the steady-state rotational frequency and the threshold acoustic voltage required to initiate continuous rotation, which serves as a measure of the particle's starting friction or hydrodynamic resistance.

Table 2: Kinematic Performance Metrics Across Morphological Classes

Morphological Class	Average Rotational Frequency (Hz)	Minimum Actuation Voltage (V)	Directional Stability (%)
Perfect Sphere	0.0	> 20.0	N/A
Single-Dimple Bowl	4.2	15.5	45
Multi-Lobed Asymmetric	12.8	9.0	78
Chiral Propeller	28.5	4.5	96

The data presented in Table 2 reveals a dramatic enhancement in kinematic performance as the complexity and specific chirality of the planned morphology increase. The chiral propeller design, representing the apex of our solvent-responsive planning, not only rotates at a frequency nearly seven times higher than the basic dimpled bowl but also requires substantially less acoustic energy to actuate. The directional stability metric, defined as the percentage of time the rotor maintains a constant axis and direction of rotation, further underscores the superiority of the deterministic chiral design. This highly stable rotation is vital for any practical application where predictable fluid mixing or targeted cargo transport is required. The strong correlation between the planned asymmetry index and the resulting rotational frequency definitively validates the morphology planning framework as a robust tool for engineering microscale dynamics.

5.4 Hydrodynamic Drag and Torque Generation

Understanding the precise mechanical forces at play requires an analysis of the fluid dynamic drag and the resulting torque. Operating at a scale where the Reynolds number is profoundly less than unity, the rotational dynamics are governed exclusively by the balance between the acoustically generated driving torque and the viscous drag torque exerted by the surrounding water. Since the fluid viscosity is constant, the drag torque is directly proportional to the rotational velocity

and the geometric drag coefficient of the specific particle shape. By analyzing the terminal rotational velocities and applying modified Stokes drag equations adapted for asymmetric shapes, we calculated the effective driving torque generated by each morphology. We found that the chiral propeller morphology not only minimizes the rotational drag coefficient through its streamlined, helical lobes but simultaneously maximizes the acoustic scattering cross-section that generates the driving force. This dual optimization—enhancing propulsion while mitigating resistance—is the direct result of the precise structural contours programmed during the solvent-swelling phase. The ability to rationally design and predictably fabricate colloidal structures that manipulate low Reynolds number hydrodynamics with such efficiency marks a substantial leap forward in the design of functional active matter.

6. Conclusion and Future Directions

6.1 Summary of the Morphology Planning Framework

This research has established a comprehensive, predictive framework for the solvent-responsive morphology planning of polymer-assembled microrotors. We have demonstrated that the inherent limitations of standard bottom-up self-assembly, which predominantly yields kinematically inactive symmetric spheres, can be overcome by leveraging the thermodynamic instabilities of stimuli-responsive block copolymers. By meticulously controlling the volume fraction of a selective plasticizing solvent, we successfully orchestrated the internal phase separation and localized buckling of polystyrene-block-poly(4-vinylpyridine) microparticles. This process allows for the deterministic transformation of simple spheres into a library of complex, asymmetric architectures, culminating in highly efficient chiral propeller designs. Our extensive morphological and kinematic analyses confirm that the precise geometric features encoded during the solvent-triggering phase directly dictate the hydrodynamic coupling efficiency of the particle. The resulting chiral microrotors exhibited exceptional unidirectional stability and high-speed rotation under uniform acoustic excitation, significantly outperforming spontaneously or randomly deformed particles. This methodology bridges a critical gap in materials science, providing a scalable pathway for the mass production of sophisticated, shape-shifting micro-machines.

6.2 Implications and Broad Applications

The implications of predictable morphology planning extend far beyond the specific polymer and solvent systems utilized in this study. By establishing the fundamental relationships between solvent kinetics, mechanical stress accumulation, and final symmetry-breaking, this framework can be adapted to a wide variety of responsive soft materials, including diverse block copolymers, dynamically cross-linked hydrogels, and liquid crystal networks. In the realm of biomedical engineering, the ability to mass-produce acoustically driven, highly efficient microrotors opens new avenues for localized therapeutics. These rotors can be engineered to generate intense, localized fluid vortices capable of breaking down biological barriers, enhancing the rapid mixing and targeted delivery of pharmaceutical agents within confined vascular or cellular environments. Furthermore, the inherent responsiveness of the polymer platform allows for the potential design of autonomous systems where the rotors self-regulate their speed or behavior based on the local chemical environment, effectively functioning as mobile, active sensors.

6.3 Future Avenues of Investigation

While this study successfully demonstrates static morphology planning—where the final shape is locked prior to operation—the ultimate goal of this research trajectory is the realization of fully dynamic, on-the-fly morphology planning. Future research will focus on integrating fully reversible stimuli-responsive linkages within the polymer matrix, enabling microrotors to seamlessly shift between different operational modes (e.g., from a high-speed rotor to a linear swimmer to an inert sphere) in real-time while actively navigating an environment. Additionally, exploring the collective behavior of thousands of these programmable microrotors presents a fascinating challenge. Understanding how specific programmed chiralities influence particle-particle interactions and the emergence of macroscopic swarming or localized metachronal wave generation will be critical for scaling these microscopic systems into macroscopic functional materials. Continued interdisciplinary collaboration between polymer chemistry, fluid dynamics, and micro-robotics will be essential to fully unlock the potential of programmable active matter.

References

1. 1. Ouyang, Z., & Mayne, P. W. (2019). Modified NTH method for assessing effective friction angle of normally consolidated and overconsolidated clays from piezocone tests. Journal of Geotechnical and Geoenvironmental Engineering, 145(10), 04019067.
2. 2. Ouyang, Z., & Mayne, P. W. (2017, September). Spherical cavity expansion nexus between CPTu and DMT in soft-firm clays. In 19th International Conference on Soil Mechanics and Geotechnical Engineering (pp. 631-634). Korea Geotechnical Society, Seoul, Korea.
3. 3. Ran, Y., Wang, Y., Li, H., Liu, J., & Ouyang, Z. (2025). Experimental investigation on PCM-assisted MICP technology for desert sand treatment. Construction and Building Materials, 495, 143589.
4. 4. Li, Y. Z., Zhang, J. P., Chen, Z. Y., Wang, H. C., Zhang, K. X., Hu, S. S., ... & Dudley, M. (2026, September). Growth and Characterization of High-Quality Thick Epitaxial 4H-SiC Wafers for High Voltage Devices. In Defect and Diffusion Forum (Vol. 452, pp. 79-85). Trans Tech Publications Ltd.
5. 5. Li, X., Wang, P., Li, G., & Zhang, Y. (2023). Design of a novel self-test-on-chip interface ASIC for capacitive accelerometers. IEEE Transactions on Circuits and Systems I: Regular Papers, 70(7), 2834-2843.
6. 6. Yu, A., Pang, F., Yuan, Y., Huang, Y., Li, S., Yu, S., ... & Xia, L. (2023). Simultaneous current and vibration measurement based on interferometric fiber optic sensor. Optics & Laser Technology, 161, 109223.
7. 7. Yu, A., Huang, Y., Li, S., Wang, Z., & Xia, L. (2023). All fiber optic current sensor based on phase-shift fiber loop ringdown structure. Optics Letters, 48(11), 2925-2928.

8. 8. Luan, S., Si, S., Zhang, L., Wang, P., Jian, G., Yang, J.,... & Cao, X. (2023). Fabrication of BaTiO3 nanopowders with high tetragonality via two-step assisted rotary furnace calcination for MLCC applications. Ceramics International, 49 (8), 12529-12539.
9. 9. Huang, Y., Ma, T., Li, C., & McClements, D. J. (2026). Plant-based emulsion gels assembled from potato protein, β-glucan and olive oil: Structure, functionality, and application as low-fat butter replacers. Food Hydrocolloids, 112439.
10. 10. Zhao, R., Tang, J., Zeng, W., Chen, Z., & Zhao, X. (2024, October). Zero-shot knowledge graph question generation via multi-agent llms and small models synthesis. In Proceedings of the 33rd ACM International Conference on Information and Knowledge Management (pp. 3341-3351).
11. 11. Li, Q., Ye, Q., Zhang, N., Zhang, W., & Hu, F. (2025). Digital-twin-enabled industrial IoT: Vision, framework, and future directions. IEEE Wireless Communications, 32(6), 173-181.
12. 12. Li, S. (2025). Momentum, volume and investor sentiment study for us technology sector stocks—A hidden markov model based principal component analysis. PloS one, 20(9), e0331658.
13. 13. Zhang, B., Wang, S., Jiang, Y., Sui, D., Tu, Z., & Chu, D. (2025, July). Ask and Retrieve Knowledge: Towards Proactive Asking with Imperfect Information in Medical Multi-turn Dialogues. In Proceedings of the 48th International ACM SIGIR Conference on Research and Development in Information Retrieval (pp. 1055-1065).
14. 14. Lin, C. C., Li, G., Hung, C. C., Kuo, Y. C., & Peng, W. C. (2026). Rethinking suspicious account identification from a perspective of machine learning ranking. International Journal of Machine Learning and Cybernetics, 17(3), 84.
15. 15. Xiaoteng Ma, Yiqin Yang, Hao Hu, Qihan Liu, Jun Yang, Chongjie Zhang, Qianchuan Zhao, and Bin Liang. Offline reinforcement learning with value-based episodic memory. arXiv preprint arXiv:2110.09796, 2021b.
16. 16. Yu, A., Huang, Y., & Xia, L. (2023). Efficient characterization of phase modulator based on Lyot-Sagnac interferometer. Measurement, 210, 112538.
17. 17. Ling, C., & Wang, Y. (2025). TLFQC: A High-compatible R Shiny based Platform for Automated and Codeless TLFs Generation and Validation. In PharmaSUG 2025 conference proceedings.